

Nucleation and Growth of Molecular Organic Crystals in a Liquid Film under Vapor Deposition

M. Voigt, S. Dorsfeld, A. Volz, and M. Sokolowski*

Institut für Physikalische und Theoretische Chemie der Universität Bonn, Wegelerstraße 12, D-53115 Bonn, Germany
(Received 19 August 2002; revised manuscript received 11 February 2003; published 11 July 2003)

We report on the nucleation and growth of tetracene in a thin liquid film which is continuously supersaturated by vapor deposition of molecules onto the film. In a first stage, nucleation and fast anisotropic two-dimensional dendritic growth occurs. In a second stage, the dendrites coarsen into pallet-shaped crystals. These are highly oriented with respect to the plane of the liquid film and reach a lateral size of several 100 μm . The two-dimensional growth mode is explained by the confined growth geometry in the liquid in combination with the anisotropy of the crystal structure.

DOI: 10.1103/PhysRevLett.91.026103

PACS numbers: 68.70.+w, 61.66.Hq, 81.15.-z

Experiments on the growth of thin solid films have been thus far mainly performed by deposition of molecules or atoms on solid substrates, and the results are discussed in the framework of classical nucleation theory [1]. We report an experiment where the material is vapor deposited into a thin *liquid* film for nucleation and subsequent coarsening of the nuclei. In particular, we have followed the crystal growth of tetracene (Tc) in a low vapor pressure liquid using *in situ* videomicroscopy. This type of experiment thus comprises aspects of the nucleation in liquids, which is commonly achieved by temperature profiles, and aspects from film growth on solid substrates, because the deposition rate can be varied deliberately. Since individual molecules are deposited onto the liquid film, the experiment allows one to vary the supersaturation level within a range not accessible by dissolving molecules in the liquid otherwise. There are two further interesting aspects of this experiment. First, due to the anisotropic character of the Tc crystal lattice and due to the quasi-two-dimensional geometry in the liquid film, the growth scenario exhibits features reminiscent of two-dimensional growth on surfaces. Second, since the diffusion length of the Tc in the liquid is large, the lateral length scales of the nucleation process, e.g., the size of the growing crystallites, is far (by about a factor of 100) beyond that which is typically found for nucleation on solid substrates. Especially this latter aspect made it possible to use optical microscopy to follow the nucleation and growth in detail, which is usually impossible for solid substrates [1].

The understanding and optimization of growth processes of organic molecular crystals in the film geometry are of particular interest. The reasons are that this geometry is required by most experiments and applications, e.g., organic field effect transistors [2], and that the achieved structural quality strongly determines the physical properties, e.g., the charge carrier mobilities [3]. Usually thin films of organic molecules are prepared by thermal vapor deposition on *solid* substrates [4]. Such films are generally microcrystalline or even amorphous with small lateral grain sizes of the order of a few μm due to a small diffusion length on the substrate surface and

incoherent nucleation of small domains [4,5]. In addition, heterogeneous nucleation at surface defects of the substrate, e.g., at steps, may play a role also. Only by a special substrate preparation, nucleation of larger molecular domains could be achieved for a specific example [6].

Under thermodynamic equilibrium, Tc crystallizes in thin pallet-shaped crystals, formed by layers of molecules oriented with their chain axis at an angle of about 70° with respect to the *ab* plane [see Figs. 1(c) and 4(c) below] [7]. The thin liquid films were prepared by spincoating bis(2-ethylhexyl) sebacate [B2EHS, see Fig. 1(a)] onto an indium tin oxide (ITO) covered glass at 5000 rpm for 30 s. The resulting film thickness was about 2–4 μm , determined from interference fringes. B2EHS is a clear liquid of low viscosity [$(22\text{--}25) \times 10^{-3} \text{ Nsm}^{-2}$ [8]] and very low vapor pressure ($< 10^{-6}$ mbar). ITO covered glass was chosen because the wetting was better on ITO compared to bare glass.

The Tc was vapor deposited onto the liquid film at room temperature ($23 \pm 2^\circ\text{C}$) from a shutter-controlled thermal evaporation source under high vacuum (1×10^{-6} mbar). The nominal deposition rates (between 0.1 and 80 nm min^{-1}) and Tc film thicknesses were measured by a quartz microbalance, calibrated by photometric measurements. Optical microscopy images were taken either subsequent to or continuously during the growth from the rear side of the transparent sample, using polarized bright field illumination. The saturation solubility of Tc in B2EHS at room temperature is 55 mg dm^{-3} (Tc:B2EHS $\approx 1:10^4$), as determined by photometric measurements. Under the plausible assumption of a sticking coefficient of Tc on the liquid surface of unity, the saturation solubility is reached for a very small nominal thickness of Tc between 0.1 and 0.2 nm, depending on the exact thickness of the liquid film.

The first interesting result is that, for deposition rates above $\sim 1 \text{ nm min}^{-1}$, Tc nucleates in large dendrites with pronounced branches (5–10 μm in width) as shown in Fig. 1(a). The growth of straight branches is a clear indication of a *dendritic* growth mode, in contrast to a *fractal* growth mode, where the branches frequently alter their directions [9]. The dendrites nucleated *in* the liquid

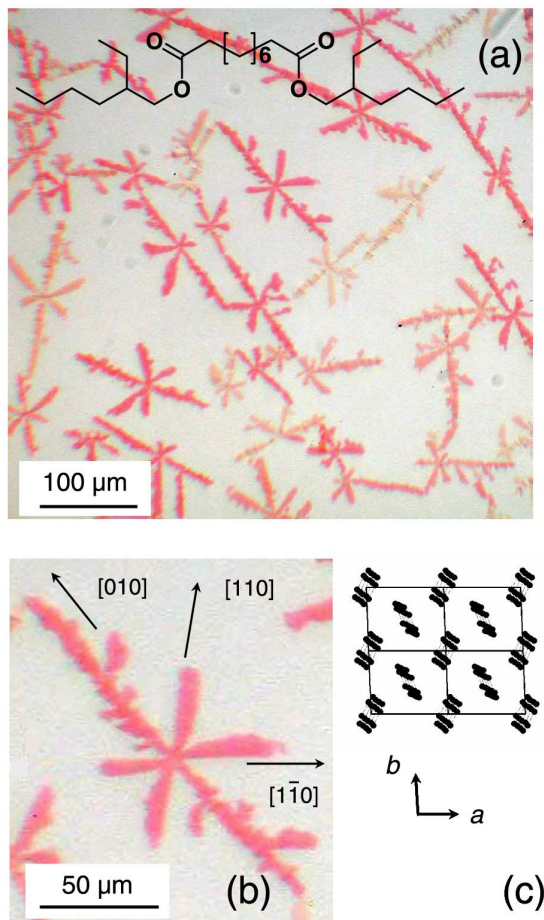


FIG. 1 (color online). Tc dendrites grown by vapor deposition onto a thin liquid film of B2EHS: (a) overview with structure formula of B2EHS and (b) individual dendrite with indicated crystal axes. Nominal Tc film thickness: 20 nm, evaporation rate: 11 nm min^{-1} . The image was taken ca. 20 min after evaporation. (c) The structure model of the *ab* plane of Tc (after Ref. [7]).

and not *on* the surface of the liquid, because they are wetted with liquid. Since the surface tension ($31.0 \pm 0.1 \text{ mN/m}$) was measured to be independent from the Tc concentration, an excess concentration of Tc on the liquid surface, forming a growth template, can be excluded. Also there are no indications of any influence of the liquid-ITO interface on the nucleation.

The dendrites are of about the same size and have a lateral extension of up to $400 \mu\text{m}$. From the deposited amount of Tc and the sample coverage ($\sim 20\%$), we derive a local thickness of about 100 nm, which is consistent with the optical absorption contrast in Fig. 1(a). However, although the dendrites exhibit a considerable thickness, the observed growth mechanism is mainly *two dimensional* and the growth fronts move fast in the plane of the liquid film. Some details of the dendritic growth are interesting in relation to the structural properties of Tc. As evident from Fig. 1(a), most dendrites ramify from their centers into two longer main branches and four shorter

main branches with well-defined angles between the branches. By comparison of the branching angles with angles between low index lattice directions in the *ab* plane of Tc [7], we conclude that most of the longer main branches are oriented along the *b* axis ([010]) and few of them are oriented along the *a* axis ([100]). For the dendrite shown in Fig. 1(b), the directions of the branches are indicated.

The crystallinity of the dendrites is also responsible for their homogenous change in color from deep orange to light yellow, which is observed if the polarizing filter in front of the illuminating light source is rotated (pleochroism). In Fig. 1(a), this is seen as a difference in the gray shades of the dendrites, depending on their orientation relative to the polarization axis. This pleochroism arises because the more intense of the two Davydov components of the optical transition in Tc crystals (at 520 nm) is polarized along the *b* axis [10] which is parallel to the plane of the liquid.

Formation of dendrites is typical for diffusion limited growth and occurs at a high level of supersaturation [9,11], which is here achieved by vapor deposition onto the liquid. Using the box counting method [11], we have estimated the fractal dimension D_f . The lowest values of D_f were observed for highest deposition rates, where the dendritic growth is most pronounced. These were between 1.33 and 1.40. The box length ε was typically varied between 2 and $100 \mu\text{m}$ and yielded good scaling (ε^{-D_f}) over about one decade in ε . This value of D_f is very small and indicates a highly anisotropic growth. Two-dimensional simulations of *isotropic* diffusion limited aggregation (DLA) [12], or experiments carried out for fractal or dendritic growth of vapor deposited atoms or molecules on surfaces [6,9], typically yield values of D_f around 1.7. Our values of D_f are considerably smaller and are even slightly below the value of 1.5 predicted from two-dimensional DLA simulations of *anisotropic* dendritic growth [13]. Anisotropic growth favors the attachment of arriving molecules at the tips of the dendritic branches and explains the formation of dominant linear backbones, as here observed. This pronounced growth speed for specific directions in the *ab* plane is presumably a consequence of a strong interaction between Tc molecules in these direction of the crystal lattice [see Fig. 1(c)].

In the second growth stage, the main branches of the dendrites coarsen into compact pallet-shaped crystallites with straight edges. This crossover from a dendritic to a compact shape occurs earlier the smaller the deposition rates are. In particular, it was possible to suppress the dendritic growth phase by starting the growth with very low deposition rates ($\sim 0.1 \text{ nm min}^{-1}$). Figure 2(a) displays a sequence taken by videomicroscopy at a deposition rate considerably smaller (1.8 nm min^{-1}) compared to that used for the pronounced dendritic growth of Fig. 1 (11 nm min^{-1}). After the nucleation, the diffusion fields of the individual dendrites start to overlap, the dendritic growth stops, and the branches coarsen into compact

pallet-shaped crystals. This second growth stage occurs with much lower lateral growth speed ($\sim 5\%$) than the growth of the dendrites, and includes an increase in crystal thickness, as visible from the enhanced contrast in Fig. 2(a).

An important issue for film growth via molecular beam deposition is the dependence of the nucleation density n_x on the deposition temperature and deposition rate R [1]. In particular, an increase $n_x \sim R^p$ is expected, whereby the exponent p depends on the dimensionality and size of the critical nucleus [1]. Figure 2(b) displays three images taken after the maximum nucleation density has been reached for R varied between 1.8 and 11.7 nm min⁻¹. The observed values of n_x increase about linear from 37 mm⁻² to 201 mm⁻², i.e., by a factor of about 5. This is in accordance with the expectation from homogenous nucleation theory and demonstrates that heterogeneous nucleation at the ITO-liquid interface can be only of minor importance. However, the precision of the data does not justify a determination of p yet. Even higher values of n_x (up to ~ 900 mm⁻²) could be obtained, if the thickness of the liquid film was reduced, e.g., by diluting B2EHS with acetone prior to spincoating, or locally close to the rim of the liquid film. This reveals again that the entire liquid film thickness is relevant for the nucleation and that the deposition rate per liquid film thickness determines the nucleation density.

Figure 3 shows the final growth stage where the dendrite branches have fully transformed into compact crystals located with partial overlap around centers, which stem from the positions of the original dendrites. All crystallites exhibit very well-defined facets. Since the crystallites are very thin, the facets on the perimeter of the crystallites are only visible as thin lines (edges) in Fig. 3. From a comparison of the angles between the edges

at the corners of the crystallites with angles between lattice lines in the ab plane of the Tc structure [7], we were able to identify the lattice directions of the edges (see Fig. 3). They are compatible with the thermodynamically stable facets observed for vapor grown Tc crystallites [14]. Therefore the crystallite shapes evolving in the second stage are thermodynamically controlled, in contrast to the kinetically controlled dendrites of the first growth stage.

From a careful inspection of the crystal shapes, two different types of crystallites (A and B) with different facets (see Fig. 3) are identified. We speculate that these stem from dendrite branches grown along the b axis (A) and other directions (B) of the Tc lattice, respectively. Remarkably, the (001) facets are always parallel to the plane of the substrate. This is concluded from x-ray diffraction data [see Fig. 4(a)], which show the series of the (00 l) Bragg reflections corresponding to the (001) plane. The reflection profiles are limited by the instrumental resolution, demonstrating a high structural order of the crystallites. The value of $d_{(001)}$ is (12.15 ± 0.02) Å, and is in agreement with the values reported for Tc single crystals within error limits [7]. The crystallites have a size that is by a factor of more than 100 larger compared to Tc crystallites grown on solid substrates, e.g., bare glass [5], which are typically only of about 1 μm in size. From rocking scans performed on the (001) Bragg reflection, a very narrow angular distribution of orientation of the crystallites with a full width at half maximum of 0.3°–0.6° is determined [see Fig. 4(b)], consistent with the possible small tilts of crystallites in the liquid film. The high structural quality of the crystallites is also deduced from their photoluminescence spectra [15] which are comparable to those of high quality vapor

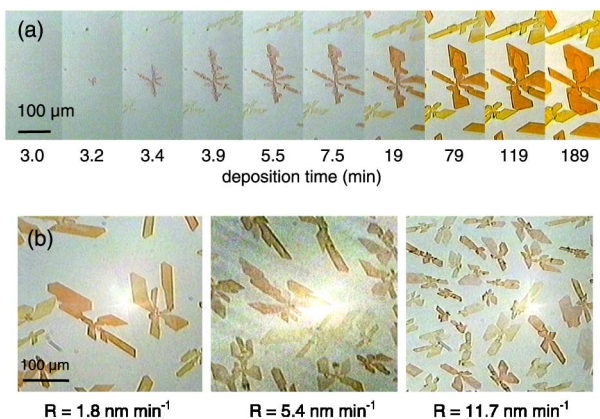


FIG. 2 (color online). Sequence of videomicroscopy images demonstrating the dendritic growth start and the subsequent coarsening of an individual Tc dendrite. The deposition rate was 1.8 nm min⁻¹. (b) Three images taken for films of the same nominal film Tc thickness (56 nm), but grown under different deposition rates. The bright spot in the middle results from stray light. For details see text.

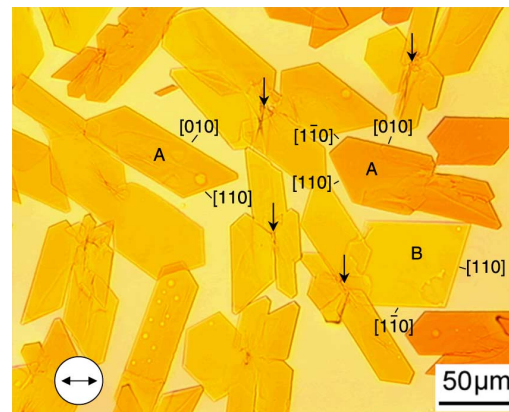


FIG. 3 (color online). Microscopic image of a Tc film at the final stage of the growth process for a nominal film thickness of 760 nm ($R = 7.4$ nm min⁻¹). For some edges of the crystallites, the lattice directions are labeled. Two types of crystallites (A, B) can be distinguished from their shape. The arrows mark centers around which several crystallites are located due to their origin from *one* dendrite. The direction of the polarization is indicated in the left bottom corner.

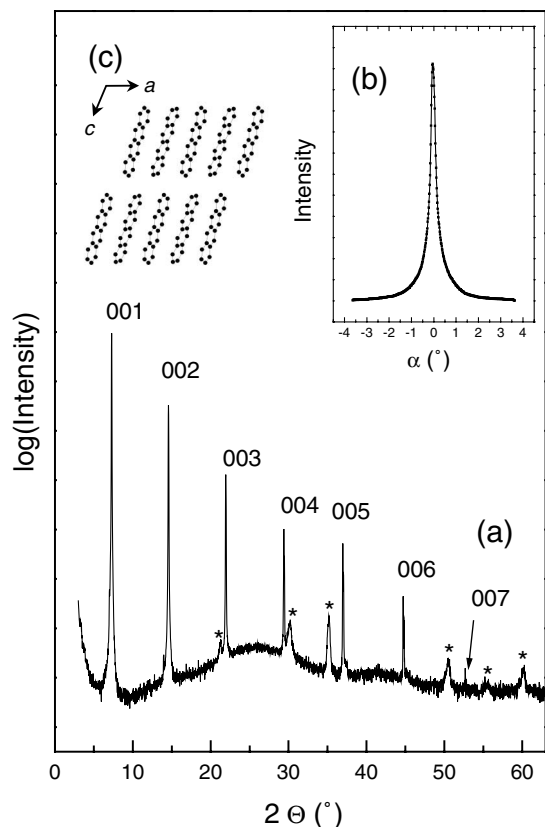


FIG. 4. X-ray diffraction scan (Bragg-Brentano geometry) of Tc crystallites grown in a thin liquid film (nominal film thickness: 430 nm) (a). The reflections corresponding to the (001) planes are numbered by their Bragg indices (00*l*). The reflections marked by an asterisk belong to the underlying ITO layer. (b) Rocking scan taken at the (001) reflection. (c) Structure model of the Tc crystal (after Ref. [7]).

grown Tc single crystals [10]. These films are thus highly attractive for optical applications, because they show no diffuse scattering of light, which is otherwise always present due to the smallness of the crystallites [5].

The growth of molecular organic crystals in thin liquid films by vapor deposition has been — to our knowledge — thus far not considered. The situation differs significantly from that of crystal growth from a saturated solution, e.g., by lowering the temperature, since in our case the liquid is *continuously* supersaturated by an *external* flux of molecules onto the liquid surface at constant temperature. The experiment which comes closest to our experiment is that of Ye *et al.* [16], who vapor deposited Ag onto a liquid film. However, there are essential differences to our experiment, since Ag clusters nucleate *on* the surface of the liquid, and since the growth of Ag fractal aggregates proceeds via cluster-cluster aggregation. In the system studied here, the solubility of the evaporated molecules *in* the liquid is important, and the diffusion field for the growth is determined by the entire liquid film and not only by processes on its two-dimensional interfaces to the substrate or vacuum. In this aspect, the here described crystal growth also differs

with respect to that described by Leiserowitz *et al.* where crystals grow from a solution at the interface to a Langmuir layer deposited onto the solution [17].

Nevertheless, the observed growth scenario exhibits features which are characteristic for growth in two dimensions. We explain this by a combination of two effects: the confined growth geometry in the liquid film which causes the diffusion field to exhibit a mainly two-dimensional character *and* a specific role of the (001) crystal facet of Tc which is oriented parallel to the growth plane due to a low sticking probability on this facet and/or its small surface energy. This latter effect is of course a consequence of the layered crystal structure of Tc [see Fig. 4(c)]. Since many molecular organic crystals also exhibit layered crystal structures, the introduced liquid-assisted two-dimensional growth scenario should have a general relevance. Indeed we recently found similar scenarios for anthracene and pentacene. Under optimized conditions, one should obtain films with large oriented crystallites for many organic materials, directly suitable for applications or preparation of high quality seed crystals.

We thank S. Hirschmann and Professor N. Karl for performing the diffraction measurements, M. Boese, S. Gericke, Dr. D. Müller, and Professors W. Mader, R. Süverkrüp, and K.-J. Steffens for experimental support, and Professor E. Umbach for the loan of equipment. The project was supported by the Deutsche Forschungsgemeinschaft.

*Corresponding author.

Electronic address: sokolowski@thch.uni-bonn.de

- [1] J. A. Venables, G. D. T. Spiller, and M. Hanbücken, Rep. Prog. Phys. **47**, 399 (1984).
- [2] G. Horowitz, Adv. Mater. **10**, 365 (1998).
- [3] N. Karl *et al.*, J. Vac. Sci. Technol. A **17**, 2318 (1999).
- [4] A. Yamashita and T. Hayashi, Adv. Mater. **8**, 791 (1996).
- [5] W. Hofberger, Phys. Status Solidi (a) **30**, 271 (1975).
- [6] F.-J. Meyer zu Heringdorf, M.C. Reuter, and R. M. Tromp, Nature (London) **412**, 517 (2001).
- [7] D. Holmes *et al.*, Chem. Eur. J. **5**, 3399 (1999), and references therein.
- [8] Merck Schuchardt, safety data sheet, issue 2000.
- [9] H. Brune *et al.*, Nature (London) **369**, 469 (1994).
- [10] K. Mizuno, A. Matsui, and G. J. Sloan, Chem. Phys. **131**, 423 (1989).
- [11] U. Bisang and J.H. Bilgram, Phys. Rev. E **54**, 5309 (1996).
- [12] T. Witten, Jr. and L. Sander, Phys. Rev. Lett. **47**, 1400 (1981).
- [13] A. Arneodo *et al.*, Phys. Rev. Lett. **66**, 2332 (1991).
- [14] E. Hertel and H.W. Bergk, Z. Phys. Chem. B **33**, 22 (1936).
- [15] M. Voigt, Diploma thesis, Universität Bonn, 2001.
- [16] G.-X. Ye *et al.*, Phys. Rev. Lett. **81**, 622 (1998).
- [17] I. Weissbuch, M. Lahav, and L. Leiserowitz, Cryst. Growth Des. **3**, 125 (2003).